# Forecast of Fluctuating Large-Scale Natural Processes and Macroscopic Correlations Effect

S.M. Korotaev and V.O. Serdyuk
Geoelectromagnetic Research Center of Schmidt Institute of Physics of the Earth, Russian Academy of Sciences(GMRC, Post Box 30, Troitsk, Moscow Region, 142190 Russia). Fax +7-495-7777218, e-mail serdyuk@izmiran.ru

**Abstract**
The macroscopic correlations effect appears as a correlation in any dissipative processes without the local carriers of interaction. In fluctuating processes there are both retarded and advanced correlations. The possibility of long-term forecasting of the random component of solar and geomagnetic activity on these advanced correlations has been investigated. The forecasting algorithm, employing advanced correlations, is suggested. Its efficiency has been proved on data of the long-term experiments in regime of the real forecast imitation with advancement up to four months. The accuracy of the obtained solar and geomagnetic forecasts is acceptable for all the practical purposes.
**Keywords:** entanglement, anticipation, forecast, Sun, geomagnetism

## 1 Introduction

In 1980 J. Cramer put forward an elegant transactional interpretation of quantum non-locality leaned upon Wheeler-Feynman action-at-a-distance electrodynamics and its generalization on quantum amplitudes [11]. He conservatively pointed out that it was the only interpretation allowed to explain all basic quantum phenomena, but did not predict any new ones [12]. However his idea proved to be much richer. Cramer was the first who explicitly distinguished the principles of strong (local) and weak (nonlocal) causality. The latter implies a possibility of advanced correlations, but only related with unknown states, or in other terms with genuine fluctuating (random) processes. The weak causality admits the extraction of information from the future without the well known classical paradoxes. It allowed Elitzur and Dolev to suggest an experimental detection of time reversed causal events [14]. Another way of account of time reversed correlation has been suggested and experimentally verified as applied to quantum teleportation by Laforest et al [42]. Although Cramer's works had some internal contradiction – the explanation of quantum phenomena on the base of classical Wheeler-Feynman theory, now the successive quantum versions of action-at-a-distance theory have been developed [18].On the other hand, as it was generally believed that quantum nonlocality existed only at the micro-level, Cramer addressed the weak causality only to this level. However the idea about persistence of nonlocality in the macroscopic limit was recently put forward from different standpoints [7, 13, 16, 17, 45] and was realized experimentally [15, 20, 46]. In addition the important experimental results were obtained before the emergence of these ideas and now have been explained as the manifestation of macroscopic entanglement [6]. The same situation turned out with N.

Kozyrev's results obtained in the framework of causal mechanics concept (and interpreted in another terms), which demonstrated phenomena very similar to macroscopic nonlocality [38], in particular, advanced correlations in the dissipative processes [39-41]. Although it is known that dissipativity has to lead to decoherence, recently the constructive role of dissipativity in entanglement generation was discovered [1, 3, 4, 10, 19]. The simplest condition for such entanglement generation is availability of a common bath (which can be served an electromagnetic field with not too restrictive properties). This way needs dissipativity of the quantum-correlated processes, namely radiation ones. Further action-at-a-distance electrodynamics [18] justifies unobservability of the advanced field and in fact the only observable result of its existence reduces to the phenomenon of radiation damping. But the latter presents a typical dissipative process. Moreover, any dissipative processes is ultimately related with radiation, and therefore with the radiation damping. The third time derivative of position appearing in the formulae of radiation damping can be directly related with the entropy production [27]. It is a reason for our next approach.

Kozyrev's works inspired us on performance of our own experiments [24, 26-36]. As a result, the availability of advanced correlations has been reliable revealed in some large-scale fluctuating dissipative astrophysical and geophysical source-processes and the probe-processes in the lab detectors which have been highly protected against the local impacts. The correlation magnitude and advancement value proved to be large. It allowed suggesting employment of this phenomenon for the forecast of such source-processes.

In this paper we present the approach of solving the forecast problem for the spontaneous component of solar and geomagnetic activity from the results of measurement of detected signals and the computation of correlations.

All presently used methods of the forecast of solar and geomagnetic activity (e.g. [2]) operate with their components determined by evolution, (even if the statistical approaches are used). However a spontaneously fluctuating, i.e. random component is rather essential. It should be stressed that we mean genuine random component (the randomness not caused by knowledge limitation about the system) It is associated with a forecasted system is complicated in a synergetic sense, the typical feature of which is instability caused by the trajectory divergence in the phase space. It is not very important only for the short-term geomagnetic forecast, because the external factors, i.e. the solar activity and interplanetary medium state are given by the observations yet. Therefore the unpredictability of many solar activity manifestations, e.g. the flares, is not of importance. But in the long-term geomagnetic forecasts which are explicitly or implicitly based on the solar activity forecast, the random component is comparable with the determined one (and exceeds it for the catastrophic events). Thus the impossibility of taking into account the random component degrades accessible accuracy and advancement of the forecasts. Therefore development of any method for the random component forecast is extremely desirable.

In Sec. 2 we discuss the heuristic model of macroscopic entanglement and related questions of causality. In Sec. 3 we present the overview of our experiments. The forecasting algorithm is presented in Sec. 4; the results of its employment are described and discussed in Sec. 5. We conclude in Sec. 6.

## 2 Theoretical Approach

Development of a successive theory of macroscopic entanglement (which has to resemble classical thermodynamics, i.e. to operate with the macroscopic parameters) is a difficult task and such theory is absent at present. But on the base of the ideas listed at the beginning of Sec. 1 the following heuristic equation of macroscopic entanglement (describing factual Kozyrev's results), relating the entropy production per particle in the probe-process in a detector $\dot{S}_d$ (dot is symbol of time derivative) and the density of total entropy production in the sources $\dot{s}$ (by Prigogine [44]) has been suggested [26, 27, 33-35]:

$$\dot{S}_d = \sigma \int \frac{\dot{s}}{x^2} \delta\left(t^2 - \frac{x^2}{v^2}\right) dV \,, \tag{1}$$

where σ is a cross-section:

$$\sigma \sim \hbar^4 / m_e^2 e^4 \,, \tag{2}$$

$m_e$ is the electron mass, $e$ is the elementary charge, $\dot{s}$ is the density of the entropy production in the sources, $x$ is distance, $t$ is time, propagation velocity $v$ for diffusion entanglement swapping can be very small, the integral is taken over the source volume. The δ-function expresses symmetrical retardation and advancement of macroscopic correlations.

Let us demonstrate a correspondence of the heuristic (1) with the strict quantum mechanical result developed for a dilute spin gas [7]. In Ref. [7], for partition of the system $A$-$B$, the following equation for the entropy of entanglement between a part $A$ and the rest of the system $B$ is obtained:

$$S_A \approx \frac{N_A N_B}{N-1} rt(2 - \log_2 e) \,, \tag{3}$$

where $N$ is the number of particles, $N = N_A + N_B$, $r$ is the collision rate.

For an adaptation of equation (1) to the conditions of the model (3), consider the steady-state regime (forget about time shift and integrate over time, neglecting the irrelevant integration constant). Then (1) reduces to:

$$S_d = \sigma \int \frac{s}{x^2} dV \,. \tag{4}$$

Consider the detector as a small part $A$ of the large homogeneous system. Correspondingly our sources prove to be the part $B$. Then:

$$S_d = \frac{S_A}{N_A} = \sigma \frac{S_B}{L^2} \,, \tag{5}$$

where $L$ is the space size of the system.

Now slightly transform (3), taking into account the assumption that the mean free path is compatible to the size of the enclosing volume [7]. That is $t = L / <v_r>$, therefore $rt = \sigma Ln$, where $n = N / V$. On the other hand, $Ln \approx N / L^2$, $rt \approx \sigma N / L^2$. Assume $N >> 1$. At last use ln (not $\log_2$) in the entropy definition (because it was always adopted in our entropy calculation [19, 20, 33-35]). As a result we can rewrite (3):

$$\frac{S_A}{N_A} \approx \sigma \frac{0.3863 N_B}{L^2} . \qquad (7)$$

We have the obvious correspondence between (5) and (7) with $S_B \approx 0.3863 N_B$. This correspondence encourages considering the equation of macroscopic entanglement (1) as at least a not too bad approximation of reality in terms of macroscopic correlations.

Eq. (1) in its simplest form does not take into account absorption by the intermediate medium. Its influence, however, is very peculiar. In Ref [18] it has been proven that although the equations of Wheeler-Feynman electrodynamics (from which the transactional interpretation is originated) are time symmetrical, the fundamental time asymmetry is represented by an absorption efficiency asymmetry: the absorption of retarded field is perfect, while the absorption of advanced one must be imperfect. It leads to the fact that level of advanced correlation through a screening medium may exceed the retarded one.

Nonlocal nature of macroscopic correlations can be tested by two ways. They both are based on the causal analysis [21-23, 24, 37]. Essentially its formalism is as follows.

For any variables $X$ and $Y$ via conditional $S(X|Y)$, $S(Y|X)$ and marginal $S(X)$, $S(Y)$ entropies (Shannon or von Neumann) the independence functions $i$ are introduced:

$$i_{Y|X} = S(Y|X) / S(Y) , \; i_{X|Y} = S(X|Y) / S(X). \qquad (8)$$

For the classical variables $0 \le i \le 1$, for the quantum ones $-1 \le i \le 1$ as the von Neumann conditional entropies can be negative [8].

Consider the classical case. Values of $i$ characterize one-sided independence of the variables. If, e.g., $i_{X|Y} = 0$ then $X$ is a single-valued function of $Y$, if $i_{X|Y} = 1$ then $X$ is independent of $Y$. Roughly speaking, values of $i$ behave inversely to module of correlation coefficient (more exactly, such analogue is $(1-i_{Y|X})(1-i_{X|Y})$). However in contrast to the correlation function, the independence ones equally fit to any (nonlinear) type of dependence $X$ and $Y$, but the main thing is they reflect asymmetry typical for causal-effect relationship. It allows introducing the causality function $\gamma$:

$$\gamma = i_{Y|X} / i_{X|Y} , \; 0 \le \gamma < \infty , \qquad (9)$$

and *to define* the cause $Y$ and the effect $X$ as variables for which $\gamma > 1$. If $\gamma < 1$, then inversely, $X$ is cause and $Y$ is effect. The case $\gamma = 1$ corresponds to adiabatic (causeless) relationship $X$ and $Y$. The described approach had been also generalized to three or more variables (the causal network, including, in particular, a common cause, common effect, causal chain and so on) [37].

The principle of strong causality is:

$$\gamma > 1 \Rightarrow \tau < 0, \qquad (10)$$

where $\tau$ is time shift of the correlation maximum $Y$ relative to $X$. Violating of (10) means signaling in reverse time, which is sufficient condition of entanglement.

Now consider the quantum case. In this case $-1 \leq i \leq 1$ and $-\infty < \gamma < \infty$ . In particular, the pure entangled state corresponds to $i_{Y|X} = i_{X|Y} = -1$. So at the quantum mechanical level the value of $\gamma$ is insufficient for distinguishing the cause and effect. We have to use for the definition of causality, instead of $\gamma$, the so-called course of time $c_2$ [22]:

$$c_2 = \frac{e^2}{\hbar} \frac{(1 - i_{Y|X})(1 - i_{Y|X}/\gamma)}{i_{Y|X}/\gamma - i_{Y|X}}. \tag{11}$$

It is the pseudoscalar velocity of causal-effect transition. The concept of the course of time was introduced by Kozyrev [38], we use his notation $c_2$, but the expression (11) is given in a modern, more complicated treatment than the original one.

Since

$c_2 < 0 \Rightarrow \gamma > 1,$ (12)

$c_2 > 0 \Rightarrow \gamma < 1,$ (13)

$c_2 \to \pm\infty \Rightarrow \gamma \to 1,$ (14)

one can use $c_2$ instead of $\gamma$ for the determination of the directionality of the causal connection. Hence a more general formulation of the principle of strong causality is:

$c_2 < 0 \Rightarrow \tau < 0,$ (15)

But as below we use only classical output of measuring device, we may employ $\gamma$ without limitations (in this we follow the accepted way of the use of Shannon entropies for proof of nonlocality [5, 9]). Notice that nonlocal correlations often are treated as instantaneous non-causal action at a distance. Our approach includes such treatment, but only as a particular limiting case (14).

Thus, calculating by experimental data $i_{X|Y}$ and $i_{Y|X}$ as a function of the time shift $\tau$ , it is possible, by their minima, to find optimal time shifts corresponding to connection of *X* and *Y*. Then, by value of $\gamma$ relative to 1, it is possible to establish the direction of the causal connection. In the case if *Y* is known to be the cause (e.g. *Y* is some measure of a source-process), while *X* is to be the effect (e.g. *X* is a detector signal), then for any classical interaction min $i_{X|Y}$ would observe only at $\tau < 0$, and this minimum would correspond to max $\gamma > 1$. Only for nonlocal transaction of *X* and *Y* it is possible $\gamma > 1$ at $\tau > 0$.

The second way is the verification of the following Bell-like inequality (the detailed derivation is presented in [31]):

$$i_{X|Z} \geq \max(i_{X|Y}, i_{Y|Z}), \tag{16}$$

where local connection of the processes *X, Y, Z* is possible only along the causal chain $Z \to Y \to X$. Violation of (16) is sufficient condition of nonlocal nature of correlation *X* and *Z*. It should be noted that in the derivation [31] of the inequality (16) the quantum property of negativity of von Neumann conditional entropies has nowhere been used. Taking into account of the parallelism of classical and quantum information theory [8] it means that the derivation holds in terms of Shannon entropies as well, so the well known usual entropic Bell inequalities do [5, 9]. Note also, that similar to usual Bell inequalities, violation of (16) does not forbid existence of *nonlocal* hidden variables. A typical hidden nonlocal variable is advanced Wheeler-Feynman field and its generalization on the quantum amplitudes [18].

## 3 Experimental Approach

As it is not possible to measure $\dot{S}_d$ and $\dot{s}$ in (1) directly, we have to evaluate for the concrete source and probe processes the theoretical expressions relating the entropies with the observables: $\dot{S}_d = F(P_d, \{p_d\})$, $\dot{s} = f(P_s, \{p_s\})$, where $P_s$ is a measured parameter of the source-process, $P_d$ is the same parameter in the probe-process (detector signal), $\{p\}$ is set of other parameters of the processes, influencing on the entropy, which must be known unless they are stable. This problem has been solved for three types of the probe-processes: spontaneous variations of weakly polarized electrodes in an electrolyte [26, 27, 30, 34, 35], spontaneous variations of dark current of the photomultiplier [27] and fluctuations of ion mobility in a small electrolyte volume [43]. The problem is quite solvable also for any source-process, though we used for quantitative verification of (1) only a rather simple example of Ohmic dissipation [24, 26, 27, 30, 34, 35].

The experiments were performed with mentioned three types of detectors. In their construction the main attention was paid to exclusion of all possible local impacts (temperature and the like). The design of the experimental setups and their parameters are described in detail in [26, 30, 34-36].

For the source-processes, the large-scale heliogeophysical processes with big random component (the solar, synoptic, geomagnetic and ionospheric activity) and the determined lab processes (phase transitions) were used. Since in the latter only retarded correlation is observed [36, 43] we do not concern them here.

The results of long-term experiments (1993 – 2003) with the heliogeophysical processes has been reviewed in [24].The main results are:

1. Signals of different detectors spaced at tens *km* turned out correlated and this correlation can not be explained by a local impact of any common factors.

2. Magnitudes of the detector signals are satisfactorily corresponding to predictions of Eq. (1).

3. The most prominent fact is reliable detection of the advanced response of the probe-processes to the all above source ones. Both inequalities (10) and (16) are violated. Maxima of the correlation functions of the detector signals and the indices of source-activity are observed at advancement of order 10 hours – 100 days and its magnitude is as much as 0.50 – 0.95. Both the advancement and correlation magnitudes increase with the source spatial scale. Advanced correlation is always more than retarded.

The main efforts has been concentrated on study of the anticipatory effect of solar and geomagnetic activity, because the former is clear cause for the latter, the former is strongest among other sources, while the latter allows the simplest computing of right-hand side of Eq. (1). Both processes have a big random component, the determined components have well known periods and therefore can be easily suppressed by filtration. It was found that detector signals have the biggest correlation with the solar radio wave flux $R$ in the frequency range 610-2800 *MHz*. Within this range an optimal frequency varies from year to year. Concerning the geomagnetic activity, it was found that detectors signals are more correlated not with local variable geomagnetic field, but with *Dst*-index of global geomagnetic activity.

For example in Fig. 1, the result of causal analysis of the solar activity $R$ (at frequency 2800 *MHz*) and electrode detector signal $U$ for a year are shown. In the advanced domain ($\tau > 0$) the values of the independence function ($U$ of $R$) are much lower than in retarded domain ($\tau < 0$) and the causality function is much more than 1. The deepest minimum $i_{X|Y} \approx 0.47$ and the highest maximum $\gamma \approx 1.6$ are observed at $\tau = 42$ days. Correlation function maximum at close $\tau$ is equal $0.76 \pm 0.08$ [26, 30].

The position of the main correlation (causal) function maximum (independence function minimum) proved to be rather instable. Although value $\tau = 42$ days turned out rather typical, it varied for different time series from 33 to 130 days.

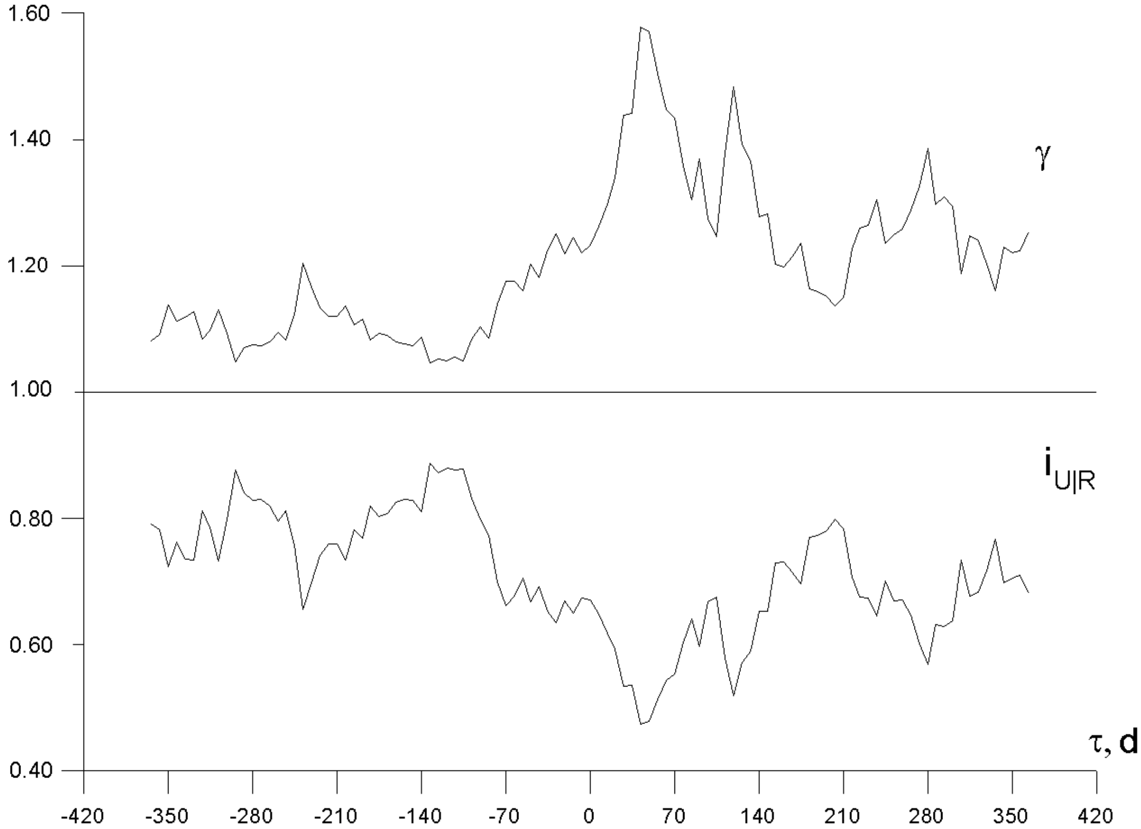


**Figure 1.** Independence $i_{U|R}$ and causality $\gamma = i_{R|U} / i_{U|R}$ functions of the detector signal $U$ and solar radio flux $R$. Negative time shift $\tau$ (days) corresponds to retardation of $U$ relative to $R$, positive one - to advancement. The realization of $U$ from 12/11/1996 to 12/10/1997 (the realization of $R$ begins 1 year before and finishes 1 year after the end of $U$).

It should be noted, that determined (periodic) components of the source-processes cause only retarded detector response. Therefore to increase the signal/noise ratio in the advanced domain one should suppress by prefiltration the main periodic components corresponding to daily, monthly (period of solar rotation) and annual variations and their harmonics. For the example of Fig.1 it turned out low-pass filtration with borderline period $T > 7$ days was enough, but, as a rule, one need to use low pass filtration $T > 28$ days or wide-band-pass filtration in the period range $28 < T < 365$ days or $28 < T < 183$ days. The band filtration is particularly important for detection of advanced correlation for the geomagnetic activity. Maximal advanced correlation with optimal prefiltration was 0.92 ± 0.03 for the solar activity [24, 28] and – 0.952 ± 0.04 for the geomagnetic one [27].

Availability of the advanced correlation allowed to demonstrate the possibility of the forecast of random component of the solar and geomagnetic activity by the detector signal by means of shift of the realizations [24, 26-30, 32, 33]. But for the real forecast in such a simplest approach fails, since, first, the processes are far from δ-correlated ones, therefore big errors are unavoidable and, second, position of the main correlation maximum is instable because of non-stationarity of the processes and one can use it only for *a posteriori* demonstration.

## 4 Practical Forecasting Algorithm

To solve the real forecast problem we have elaborated a method based on the convolution of impulse transfer characteristic with multitude of the preceding detector signal values. On the "training" interval $[t_1, t_2]$ we compute the impulse transfer characteristic $g(\tau)$, which relates the detector signal $X$ and the forecasted parameter $Y$, by solving the following equation:

$$Y(t) = \int_{t_1}^{t_n} g(\tau)X(t-\tau)d\tau \ . \tag{17}$$

The solution of Eq. (17) in the discrete form is reduced to the system of linear equations $\{\boldsymbol{Y}=\boldsymbol{XK}\}$. The components of $\boldsymbol{K}$ vector are equivalent to coefficients of plural cross-regression (for the case of eigendistribution). The number of equations $n$ equals to the advancement of the forecast. $\boldsymbol{X}$ is the square matrix $n\times n$, the rows are formed from values of the detector signal on the training interval. The first row consists of the values with time index from 1 to $n$, the second – from 2 to $n$+1, etc. The sequential values of the $Y$ are corresponding to the each row of matrix. The system is solved with the Gauss method. The stability of the results is achieved by an optimal regularization. Practically the advancement is chosen to be equal to the expected average position of the maximum correlation. The total training interval for $Y$ ends by the last observed value, while for $X$ – preceding on $\Delta t$.

The transfer characteristic computed in such a way is then used for the calculation of the only value of the forecasted parameter $Y$ with the advancement $\Delta t$. For this purpose the direct problem (17) is solved by $X$ interval ended by the last observed value. On the next step (day) the training interval moved forward and the next value $Y$ is forecasted.

Such procedure allows minimizing influence of non-stationarity. To suppress the residual instability the received sequence goes through an optimal low-pass postfiltration.

This method is more preferential then those often employed in the analogous situation (of uncertainty of the cross-correlation function maximum) the plural regression method on correlation matrix calculation, since the suggested one does not require any additional hypothesis about the probability distribution. It is essential, for the reason that distribution very seldom is the eigendistribution. But the latter is needed for uniqueness of the regression problem traditional solution. In addition the distribution is not nearly always Gaussian, what is needed for correspondence of this solution to the maximal likelihood criterion.

Note that Eq. (17) is rather universal and convenient for solving of the anticipatory problem in question, but it could apply to an ordinary deterministic forecast. Hence the algorithm is called pragmatic. But physically there is difference of principle in directionality of causal connection: in our method $Y \rightarrow X$, while in any customary ones $X \rightarrow Y$. Namely time reversal allows to forecast fluctuating processes.

# 5 Results of the Experimental Forecasts

The algorithm described in Sec 4 has been tested on data previously collected in our experiments, but we have done it, simulating the forecast in real time. We have employed all obtained detector signal hourly time series of sufficient length – not less than one year for the solar radio flux *R* and two years for the geomagnetic activity *Dst* (because of shortcoming of the series length, especially valuable with wide-band prefiltration necessary for *Dst*). Only the data of the electrode detector *U* (which proved to be the most technically reliable) have satisfied this requirement.

Results of day by day forecasting were compared with factual evolution of *R* or *Dst*. Quality of the forecast was assessed by standard deviation of the forecasting and factual curves ε (absolute error in corresponding units, i.e. $10^{-22}\ Wm^{-2}Hz^{-1}$ for *R* and *nT* for *Dst*). Certainly, both the curves were taken after the same prefiltration.

According to the algorithm, every point of forecasted curves presented below is the result of a computation by selected observed data, the minimal volume of which is determined by the forecast advancement (determining duration of the training interval) and by the filter parameters. It should be stressed that we have restricted ourselves to the forecasts of only the long-period random component, which is the background forecasts, although the macroscopic correlation effect in itself admits the forecast of individual powerful events [32].

## 5.1 The Solar Forecasts

In Fig. 2 the solar forecast (*R* at 2800 *MHz*) with the same data and with the same prefiltration ($T > 7$ days) as for Fig. 1 is shown. This is time (1997) of beginning of the next in turn solar cycle. As it is well known, 11 years is only a mean value of the cycle period, the moment of a cycle beginning (i.e. the increase after a minimum) is a random event. It is interesting to test the capability of the method around this time. Namely for this reason prefiltration for this case is only $T > 7$ days. The forecasting curve was post-filtered also with $T' > 7$ days. Resulting advancement $\Delta t = 39$ days and error $\varepsilon = 5.2$ are only slightly less than without postfiltration: $\Delta t = 42$ days, $\varepsilon = 5.4$. It can be seen that the cycle beginning (the sharp increase of $R$ at 125 $d$) is well predicted.

In Fig. 3 the solar forecast ($R$ at 610 $MHz$) by the longest available time series is shown. Prefiltration in this case was $T > 28$ days, postfiltration – $T' > 14$ days. Resulting advancement $\Delta t = 35$ days, error $\varepsilon = 0.88$, while without postfiltration $\Delta t = 42$ days, $\varepsilon = 1.16$. In this case there is a clear utility of postfiltration.

In Fig. 4 the solar forecast ($R$ at 1415 $MHz$) by data of the most recent (2001 – 2003) experiment provided the most advancement is shown. Prefiltration was $28 < T < 183$ days, postfiltration – $T' > 14$ days. Resulting $\Delta t = 123$ days, $\varepsilon = 2.0$. Without post-filtration $\Delta t = 130$ days, $\varepsilon = 2.4$.

A few examples, of course, do not allow a certain concluding about statistical dependence of the error $\varepsilon$ on the advancement $\Delta t$. But it is clear that some minimum $\varepsilon(\Delta t)$ must exist, corresponding to a mean position of maximum $\gamma(\Delta t)$, i.e. an optimal advancement must be for such a forecast.

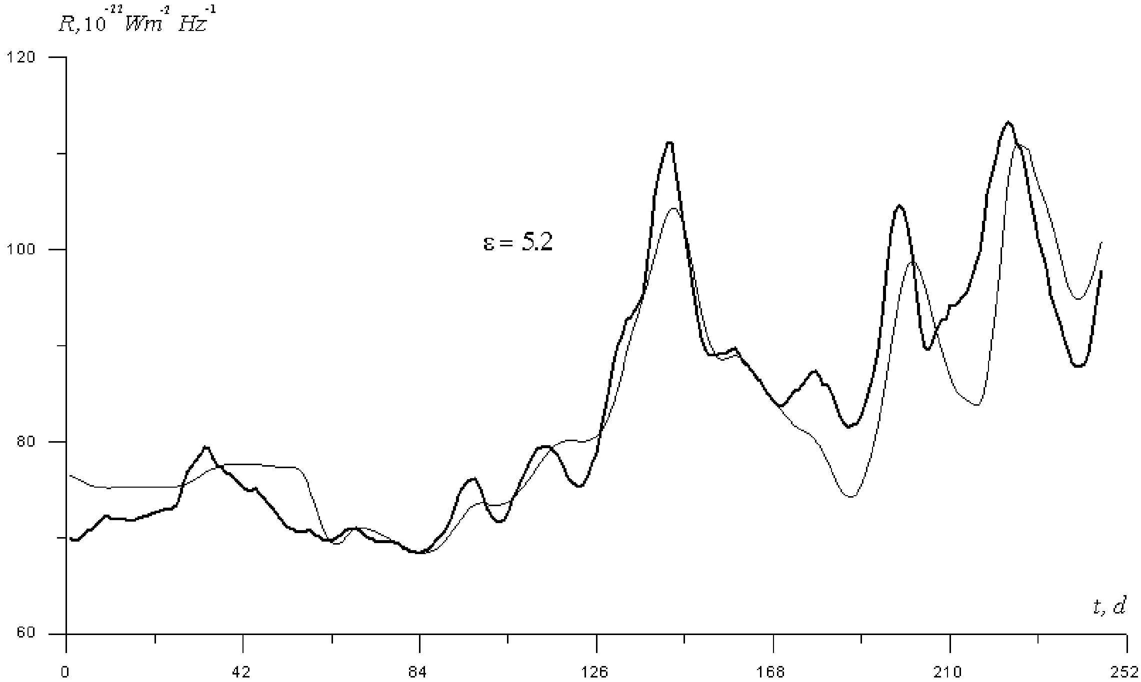


**Figure 2.** The forecast of solar activity with advancement 39 days (fine line) compared to the factual curve (thick line). The origin of time count (days) corresponds to 3/21/1997.

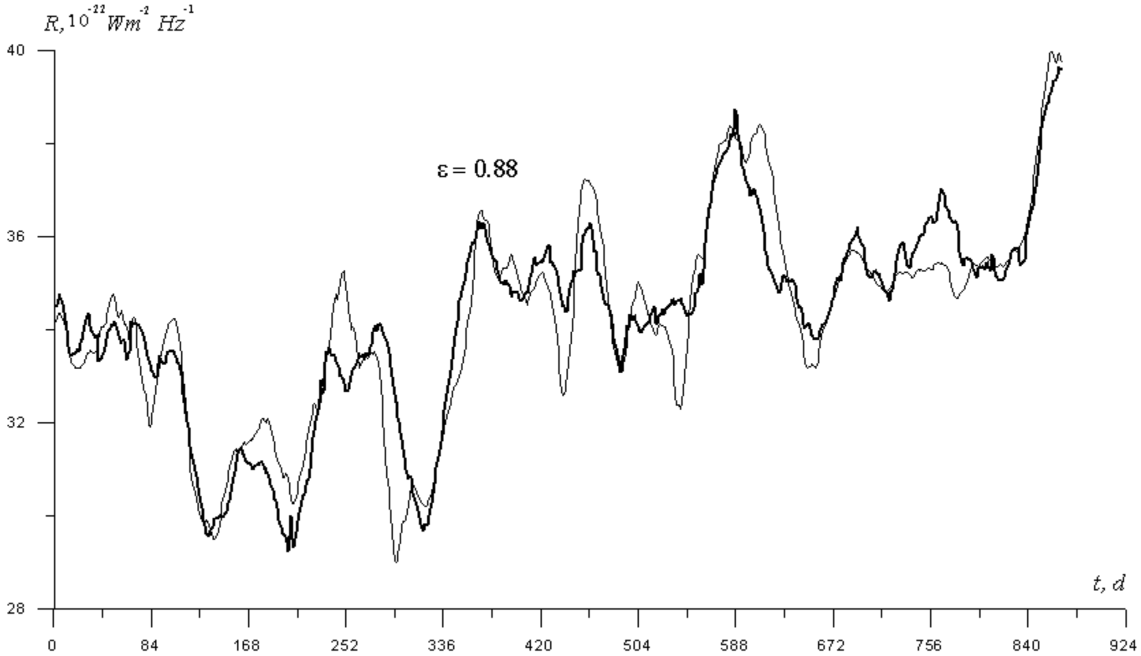


**Figure 3.** The forecast of solar activity with advancement 35 days compared to the factual curve. The origin of time count corresponds to 3/20/1995.

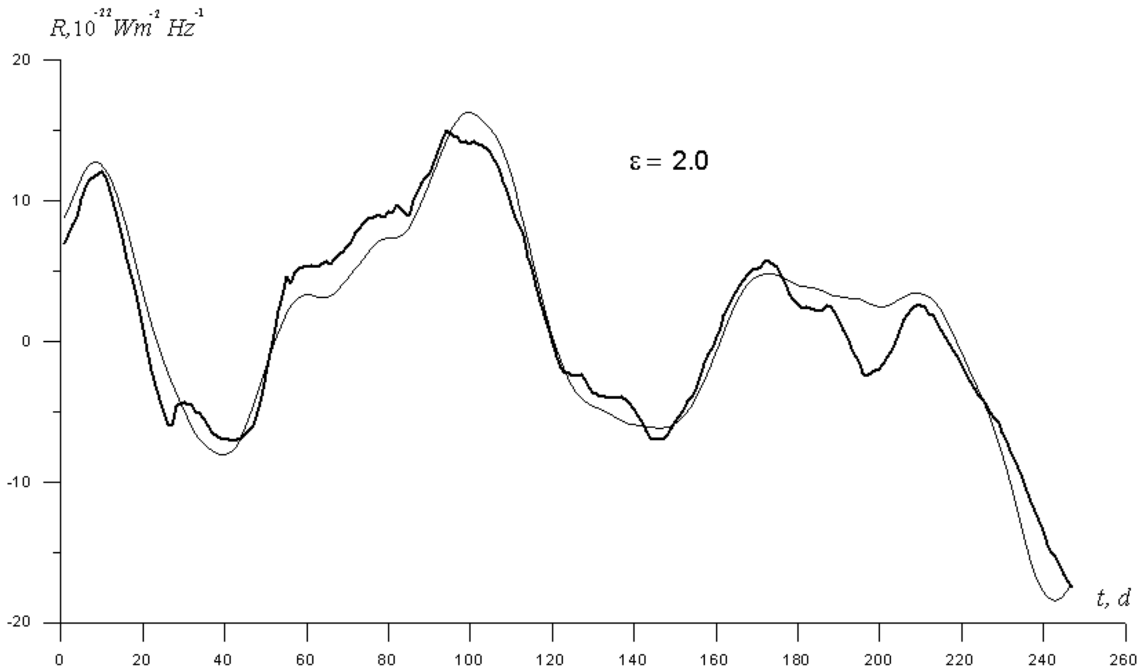


**Figure 4.** The forecast of solar activity with advancement 123 days compared to the factual curve. The origin of time count corresponds to 2/20/2003.

## 5.2 The Geomagnetic Forecasts

In Fig. 5 the geomagnetic forecast (*Dst*-index) by the same detector data (that is by the longest experimentally obtained time series) and with the same postfiltration as for Fig 3. (but with another prefiltration $28 < T < 364$ days to suppress the specific deterministic component of geomagnetic activity) is shown. Resulting advancement of the forecast $\Delta t = 35$ days, error $\varepsilon = 1.7$. Without postfiltration $\Delta t = 42$ days, but $\varepsilon = 2.4$.

In Fig. 6 the geomagnetic forecast (*Dst*-index) by the same data and with the same pre- and postfiltration as for Fig. 4 is shown. Resulting $\Delta t = 123$ days, $\varepsilon = 2.9$, while without postfiltration $\Delta t = 130$ days, $\varepsilon = 3.5$.

It is well known that geomagnetic activity is a direct effect of solar one. The retardation of geomagnetic activity relative to solar one equals about 1 day (maximum 2 days) that is insignificant in our time scale. Therefore the advancement of correlation of the both processes with the detector signal is practically equal [17]. Hence the optimal advancement for the solar and geomagnetic forecasts by the same time series of the detector signal turns out the same (the pairs shown in Figs. 3 and 5, and in Figs. 4 and 6).

It is well known also that, in spite of the clear causal connection, the correlation coefficient of solar and geomagnetic activities is rather small (of order – 0.3 in terms of *R* and *Dst*, e.g. [21]). Under this condition, an equal success of the solar and geomagnetic forecasts (their accuracy is acceptable for all the practical purposes) means that the detector signal contains direct information about the both activities. Probably it is an sequence of bipartite nature of the macroscopic entanglement of three biseparable states.

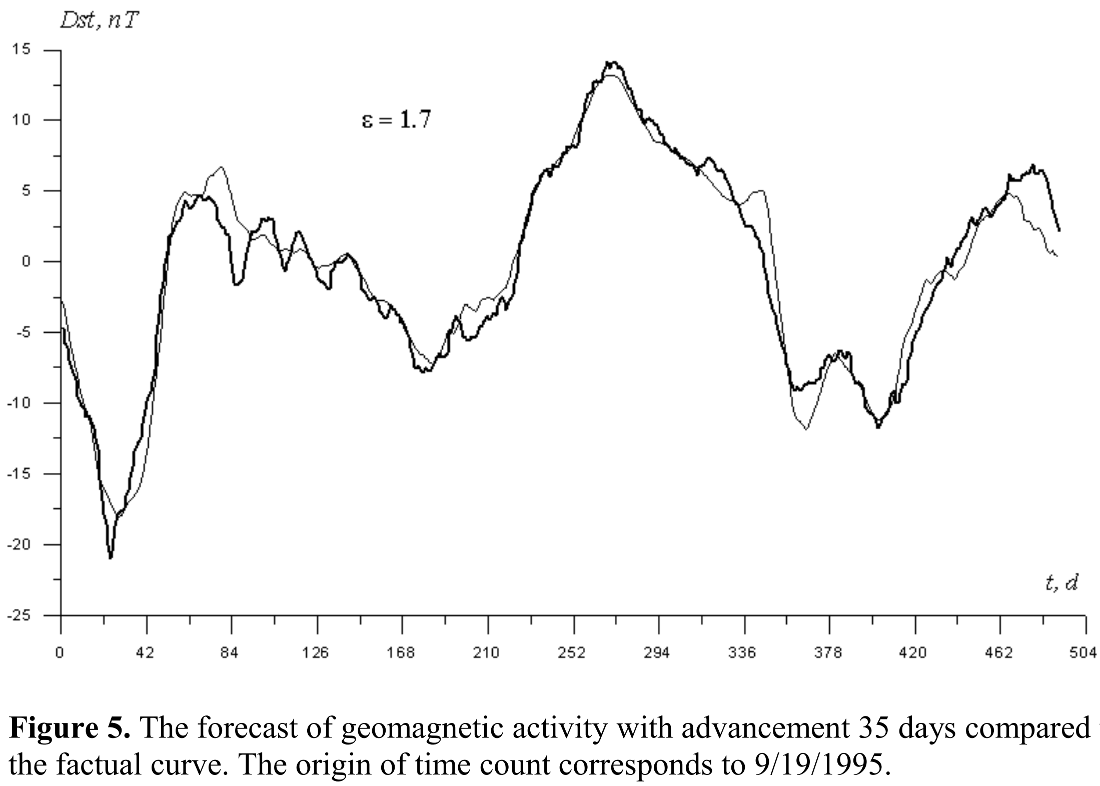


**Figure 5.** The forecast of geomagnetic activity with advancement 35 days compared to the factual curve. The origin of time count corresponds to 9/19/1995.

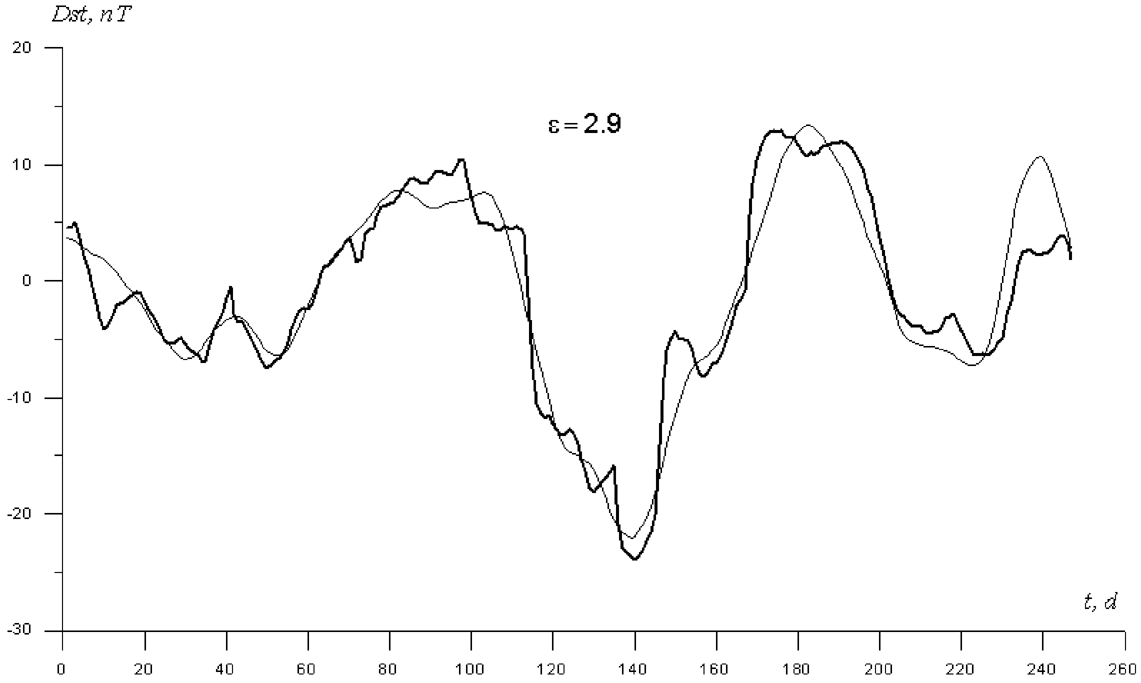


**Figure 6.** The forecast of geomagnetic activity with advancement 123 days compared to the factual curve. The origin of time count corresponds to 2/20/2003.

## 6 Conclusion

We have presented a theoretical and an experimental approach to the anticipatory effect of macroscopic correlations. The former is rather heuristic, while the latter is quite rigorous. The availability of fairly strong advanced correlations with large value of advancement enables us to put and solve the problem of forecasting of random large-scale natural processes on the macroscopic correlations effect. We have considered this problem as applied to the solar and geomagnetic activities. The pragmatic forecasting algorithm on the macroscopic correlations has been developed. Its efficiency has been proved on all data of the long-term experiments in regime of the real forecast imitation with advancement up to four months.

It should be stressed that the suggested method is unique namely by the possibility of forecasting of the spontaneous (random) component of fluctuations. All existing approaches to the forecasting problem are deterministic (in spite of employment of statistical cross- or auto-regression algorithms), the random component is an unavoidable error for them. Indeed a true random process can not be forecasted by any classical way. Namely quantum nature of the macroscopic correlations effect has allowed forecasting such processes. Therefore the described method is essentially complementary to the customary ones.

It stands to reason that the development of the theory of macroscopic entanglement, especially in the action-at-a-distance electrodynamics spirit, has a fundamental importance. Perhaps our theoretical approach is too rough. But regardless of the interpretation, the accuracy of the obtained solar and geomagnetic forecasts is acceptable for all the practical purposes.

## References


[1] Basharov A.M. (2002) Decoherence and Entanglement by Radiation Decay of Two-Atom System: J. Experimental and Theoretical Phys. V. 121, pp.1249-1260.

[2] Belov A.V., Gaidash S.P., Kanonidi Kh.D., Kanonidi K.Kh., Kuznetsov V.D. and Eroshenko E.A. (2005) Operative Center of the Geophisycal Prognosis in IZMIR-AN: Annales of Geophysicae, V.23 (9), pp. 3163-3170.

[3] Benatty F., Floreanini R. and Piani M. (2003) Environment Induced Entanglement in Markovian Dissipative Dynamics: Phys. Rev. Lett.. V. 91, pp. 070402-1-4.

[4] Braun D. (2002) Creation of Entanglement by Interaction with a Common Heat Bath: Phys. Rev. Lett. V. 89, pp. 277901-1-4.

[5] Braunstain S.L. and Caves C.M. (1988) Information-Theoretic Bell Inequalities: Phys. Rev. Lett. V. 61, pp. 662-665.

[6] Brucner C., Vedral V. and Zeilinger A. (2006) Crucial role of Quantum Entanglement in Bulk Properties of Solids: Phys. Rev. A. V.73, pp. 012110-1-4.

[7] Calsamiglia J., Hartmann L., Dur W. and Briegel H.-J. (2005) Spin Gases: Quantum Entanglement Driven by Classical Kinematics: Phys. Rev. Lett. V. 95, pp. 180502-1-4.

[8] Cerf N.C. (1998) Entropic Bounds on Coding for Noisy Quantum Channels: Phys. Rev. A. V. 57, pp.3330-3347.

[9] Cerf N.C. and Adami C (1997) Entropic Bell Inequalities: Phys. Rev. A. V. 55, pp. 3371-3374.

[10] Choi T. and Lee H. (2007) Quantum Entanglement Induced by Dissipation: Phys. Rev. A. V. 76, pp. 012308-1-5.

[11] Cramer J.G. (1980) Generalized Absorber Theory and Einstein-Podolsky-Rosen Paradox: Phys. Rev. D. V. 22, pp. 362-376.

[12] Cramer J.G. (1986) The Transactional Interpretation of Quantum Mechanics: Rev.-Mod. Phys. V. 58, pp. 647-688.

[13] Dur W. and Briegel H.-J. (2004) Stability of Macroscopic Entanglement under Decoherence: Phys. Rev. Lett. V. 92, pp. 180403-1-4.

[14] Elitzur A.S. and Dolev S. (2003) Is there more to T?: The Nature of Time: Geometry, Physics and Perception. Edited by R. Buccery, M. Saniga and W.M. Stuckey, Kluwer Academic Publishers, pp. 297-306.

[15] Ghosh S., Rosenbaum T.F., Aepll G.A. and Coppersmith S.N. (2003) Entanglement Quantum State of Magnetic Dipoles: Nature. V. 425, p.48.

[16] Hein M., Dur W. and Briegel H.-J. (2005) Entanglement Properties of multipartite entangled states under influence of decoherence: Phys. Rev. A. V. 71, pp. 032350-1-25.

[17] Home D. and Majumdar A.S. (1995) Incompatibility Between Quantum Mechanics and Classical Realism in the Strong Macroscopic Limit: Phys. Rev. A. V 52, pp. 4959-4962.
[18] Hoyle F. and Narlikar J.V. (1995) Cosmology and Action-at-a-Distance Electrodynamics: Rev. Mod. Phys. V. 67, pp. 113-156.
[19] Jakobczyk L. (2002) Entangling Two Qubits by Dissipation: J. Phys. A. V. 35, pp. 6383–6391.
[20] Julsgaard B., Kozhelkin A. and Polsik E.S. (2001) Experimental Long Lived Entanglement of Two Macroscopic Objects: Nature. V. 413, pp. 400-403.
[21] Korotaev S. M. (1992) On the Possibility of Causal Analysis of the Geophysical Processes: Geomagnetism and Aeronomy. V. 32, pp. 27-33.
[22] Korotaev S. M. (1993) Formal Definition of Causality and Kozyrev's Axioms: Galilean Electrodynamics. V.4 (5), pp.86–89.
[23] Korotaev S.M. (1995) Role of Different Definitions of the Entropy in the Causal Analysis: Geomagnetism and Aeronomy. V. 35, pp. 116-125.
[24] Korotaev S.M. (2006) Experimental Study of Advanced Correlation of Some Geophysical and Astrophysical Processes: Int. J. of Computing Anticipatory Systems. V. 17, pp. 61-76.
[25] Korotaev S.M., Hachay O.A. and Shabelyansky S.V. (1993) Causal Analysis of the Process of Horizontal Informational Diffusion of Electromagnetic Field in the Ocean: Geomagnetism and Aeronomy. V. 33, pp. 128-133.
[26] Korotaev S.M., Morozov A.N., Serdyuk V.O. and Gorohov J.V. (2003) Experimental Evidence of Nonlocal Transaction in Reverse Time: Physical Interpretation of Relativity Theory. Edited by M.C. Duffy, BMSTU Press, pp. 200-212.
[27] Korotaev S.M., Morozov A.N., Serdyuk V.O., Gorohov J.V. and Machinin V.A. (2005) Experimental Study of Macroscopic Nonlocality of Large-Scale Geomagnetic Dissipative Processes: NeuroQuantology. V. 3, pp. 275-294.
[28] Korotaev S.M., Morozov A.N., Serdyuk V.O., Gorohov J.V., and Machinin V.A. (2005) Experimental Study of Advanced Nonlocal Correlation of Large Scale Dissipative Processes: Physical Interpretation of Relativity Theory. Edited by P. Rowlands, BMSTU PH, pp. 209 – 215.
[29] Korotaev S.M., Morozov A.N., Serdyuk V.O., Nalivayko V.I., Novysh A.V., Gaidash S.P., Gorohov J.V., Pulinets S.A. and Kanonidi Kh. D. (2004) Manifestation of macroscopic nonlocality in the processes of solar and geomagnetic activity: VESTNIK Journal of Bauman Moscow State Technical University. Special Issue, pp. 173-185.
[30] Korotaev S.M., Morozov A.N., Serdyuk V.O. and Sorokin M.O. (2002) Manifestation of Macroscopic Nonlocality in Some Natural Dissipative Processes: Russian Phys. J. V. 45 (5), pp. 3-14.
[31] Korotaev S.M., Serdyk V.O. and Gorohov J.V. (2007) Forecast of Solar and Geomagnetic Activity on the Macroscopic Nonlocality Effect: Hadronic Journal. V. 30 (1), pp. 39-56.

[32] Korotaev S.M., Serdyuk V.O., Gorohov J.V., Pulinets S.A. and Machinin V.A. (2004) Forecasting Effect of Macroscopic Nonlocality: Frontier Perspectives. V. 13 (1), pp. 41-45.
[33] Korotaev S.M., Serdyuk V.O., Nalivaiko V.I., Novysh A.V., Gaidash S.P., Gorokhov Yu.V., Pulinets S.A. and Kanonidi Kh.D. (2003) Experimental Estimation of Macroscopic Nonlocality Effect in Solar and Geomagnetic Activity: Phys. of Wave Phenomena. V. 11 (1), pp.46-55.
[34] Korotaev S.M., Serdyuk V.O. and Sorokin M.O. (2000) Effect of Macroscopic Nonlocality on Geomagnetic and Solar-Ionospheric Processes: Geomagetism and Aeronomy. V. 40, pp. 323-330.
[35] Korotaev S.M., Serdyuk V.O., Sorokin M.O. and Abramov J.M. (1999) Geophysical Manifestation of Interaction of the Processes Through the Active Properties of Time: Phys. and Chem. of the Earth A. V.24, pp. 735-740.
[36] Korotaev S.M., Serdyuk V.O., Sorokin M.O. and V.A. Machinin (2000) Experimental study of nonlocality of the controlled dissipative processes: Physical Thought of Russia No 3, pp. 20-26.
[37] Korotaev S.M., Shabelyansky S.V. and Serdyuk V.O. (1992) Generalized Causal Analysis and its Employment for Study of Electromagnetic Field in the Ocean: Izvestia Physics of the Solid Earth. No 6. pp. 77-86.
[38] Kozyrev N.A. (1971) On the Possibility of Experimental Investigation of the Properties of Time: Time is Science and Philosophy. Edited by J. Zeman, Academia, p.111-132.
[39] Kozyrev N.A. (1980) Astronomical Proofs of Reality of 4D Minkowski Geometry: Manifestation of Cosmic Factors on the Earth and Stars. Edited by A.A. Efimov, VAGO Press, pp. 85-93.
[40] Kozyrev, N.A. and Nasonov, V.V. (1978) New Method of Determination of Trigonometric Parallaxes on the Base of Difference Between Actual and Visible Position of the Stars: Astrometry and Heavenly Mechanics. Edited by A.A. Efimov, VAGO Press, pp. 168-179.
[41] Kozyrev, N.A. and Nasonov, V.V. (1980) On Some Properties of Time Revealed by Astronomy Observations: Manifestation of Cosmic Factors on the Earth and Stars. Edited by A.A. Efimov, VAGO Press, pp.76-84.
[42] Laforest M., Baugh J. and Laflamme R. (2006) Time-reversal Formalism Applied to Bipartite Entanglement: Theoretical and Experimental Exploration: Phys. Rev. A. V. 73, pp. 032323-1-8.
[43] Morozov, A.N. (1997) Irreversible Processes and Brownian Motion. Published by BMSTU Press: Moscow.
[44] Prigogine I. (1979) From Being to Becoming. Published by W.H. Freeman & Co.
[45] Simon C. and Kempe J. (2002) Robustness of Multiparty Entanglement: Phys. Rev. A. V.65, pp. 052327-1-4.
[46] Xu H., Strauch F.W., Dutta S.K., Johnson P.R., Ramos R.C., Berkley A.J., Paik H., Anderson J.R., Dragt A.J., Lobb C. J. and Wellstood F.C. (2005) Spectroscopy of Three-Particle Entanglement in a Macroscopic Superconducting Circuit: Phys. Rev. Lett. V. 94, pp. 027003-1-4.